Single-Layer Feed Waveguide Consisting of Posts for Plane TEM Wave Excitation in Parallel Plates

Jiro Hirokawa, *Member, IEEE*, and Makoto Ando, *Member, IEEE*

***Abstract*—The authors propose a novel feed structure to excite a plane TEM wave in a parallel-plate waveguide. The feed waveguide is composed of densely arrayed posts on the same layer as the parallel plate. The posts can be easily fabricated at low cost by making metalized via holes in a grounded dielectric substrate. Such a procedure results in a quite simple fabrication of the antenna. The feed waveguide is designed to obtain a uniform division, which is confirmed by measurements on a 40-GHz band model.**

***Index Terms*—Parallel-plate waveguides.**

I. Introduction

A parallel-plate slot array antenna is an attractive candidate for high-efficiency and mass-produceable planar phased-array antennas [1], [2] for millimeter-wave applications. In general, the transmission loss in a waveguide is very small in comparison with other feedlines such as a microstrip line and a suspended line. The radiating part has a simple structure that consists of slots etched on the upper plate. A number of various techniques to excite a plane TEM wave in the parallel-plate waveguide have been reported in the literature [3]–[10]. Feed structures using a horn [7] and a parabolic reflector [8] are simple, but need relatively large areas when placed on the same layer as the radiating parts. In order to reduce the antenna size, the feed structure should be attached to the bottom of the radiating part and connected to it by a bend. A feed structure using a nonradiative dielectric (NRD) guide [9] raises the same problem since it is difficult to provide radiation in the direction perpendicular to the guide. The authors previously proposed a waveguide-fed parallel-plate slot array antenna [10] in which a rectangular feed waveguide was attached to the bottom of the parallel-plate waveguide. These feed structures are a bit complicated from the manufacturing point of view.

In this paper, we introduce a novel single-layer structure for a feed waveguide, as shown in Fig. 1. The walls of the waveguide are equivalently composed by densely arrayed posts. The structure is advantageous in terms of practical fabrication of planar antennas for millimeter-wave applications such as wireless LAN (59–60 GHz) and car collision avoidance radar (76.5–77.5 GHz). For example, the antenna can be easily fabricated at low cost by making many via holes in a grounded dielectric substrate and metalizing them as posts. Section II explains the structure and the operational principle of the single-layer feed waveguide exciting a plane TEM wave in a parallel-plate waveguide. In Section III, we analyze the propagation constant of a waveguide consisting of posts (called thereafter a post-wall waveguide) as a function of their spacing and diameter. Section IV presents a moment-method analysis of a unit component of the feed waveguide (named a periodic-wall π junction), while Section V shows the characteristics of the component. Next, the design procedure of the feed waveguide to obtain uniform power division is described in Section VI. Section VII confirms the uniform division of the feed waveguide by measurements on a 40-GHz band model. In Section VIII, we present problems that still have to be solved in a future study. Finally, Section IX is devoted to summarizing the results presented in this paper.

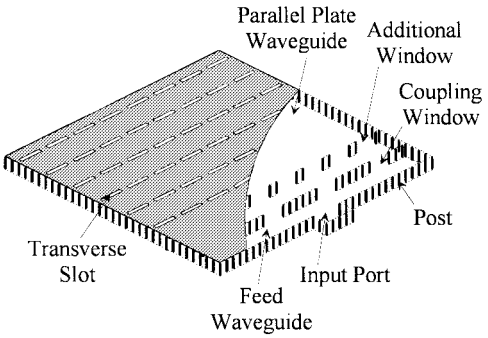

Fig. 1. Parallel-plate slot array with a single-layer feed waveguide.

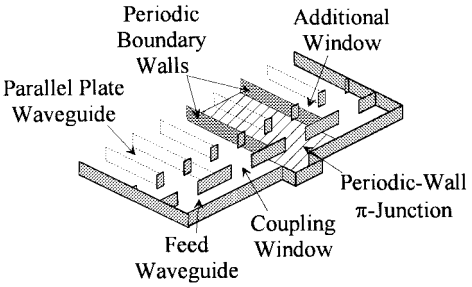

Fig. 2. Single-layer feed waveguide to excite plane TEM wave.

II. Structure

Fig. 2 shows the configuration of the structure based on the feed waveguide of a single-layer slotted waveguide array [11], [12]. It is placed on the same layer as the radiating rectangular

Manuscript received April 30, 1997; revised October 7, 1997.

The authors are with the Department of Electrical and Electronic Engineering, Tokyo Institute of Technology, Meguro-ku, Tokyo 152-8552, Japan.

Publisher Item Identifier S 0018-926X(98)03368-7.

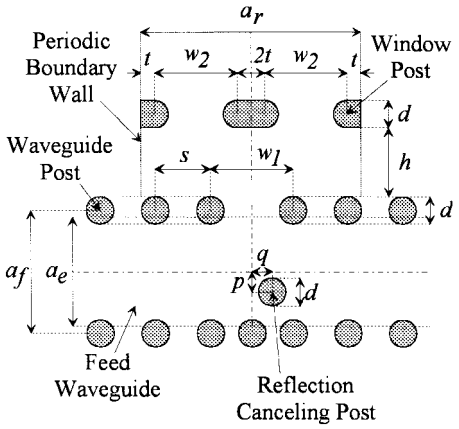

Fig. 3. Periodic wall π junction consisting of posts.

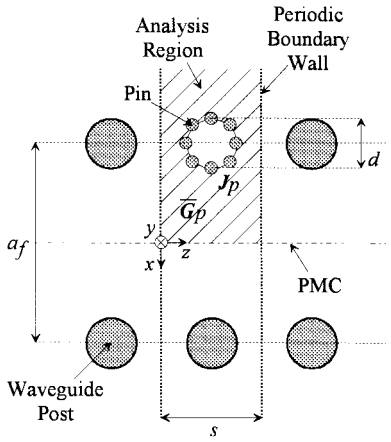

Fig. 4. Analysis model of a post-wall waveguide.

waveguides and arranged as a cascade of π junctions. A π junction has a window to couple with two radiating waveguides in phase when the width of the feed waveguide is set so that the guide wavelength of the feed waveguide is twice as long as the width of the radiating waveguide. The feed waveguide is two-dimensional (2-D) and uniform along the height with an input port placed at its center. If all the walls of the radiating waveguides are eliminated, undesired waves can propagate obliquely in two directions (except for desired propagation in boresight direction) since the spacing of the coupling windows is longer than a guide wavelength in the radiating waveguide region (parallel-plate waveguide). Two additional windows should be placed in front of each coupling window to eliminate the undesired propagation as shown in Fig. 2 [13]. In practical fabrication of the antenna, the walls will be replaced with densely arrayed posts.

When the coupling windows are designed to divide an input power in equal amplitude and phase, the field in the parallel-plate waveguide becomes periodical in the transverse z direction with the period of the coupling window. A unit component (called periodic-wall π junction) can be separated to design the coupling windows by assuming two periodic boundary walls, as shown in Fig. 2 [14]. Fig. 3 represents a product model of the periodic-wall π junction. As can be seen, an additional post placed in front of the coupling window in the feed waveguide cancels the reflection from the window. The structure of the periodic-wall π junction is symmetrical with respect to the center of the coupling window, except for the reflection-canceling post. The two additional windows have the same width w_2. The waveguide posts in Fig. 3 are replaced by perfect electric conductor (PEC) walls with thickness of the post diameter d.

III. Propagation Constant of a Post-Wall Waveguide

It is important to estimate the width a_f of the post-wall feed waveguide as a function of the spacing s and the diameter d of the posts to get the same propagation constant as the dominant mode in the PEC wall waveguide of width a_e. Fig. 4 shows an analysis model of the post-wall waveguide. The structure is 2-D and uniform along the y direction. The posts are arrayed infinitely with a period s along the z direction. This analysis calculates the wavenumber k_{zd} along the z direction of the dominant TE-to-z mode in which E_z is symmetrical with respect to the $x = 0$ plane. A perfect magnetic conductor (PMC) wall can be assumed at the $x = 0$ plane. Therefore, only one post is considered in the analysis region as shown in Fig. 4. Several uniform electric currents $\boldsymbol{J}_{pj}(j = 1 - I_p)$ with only the y component are assumed on the post surface [15], [16]. By using the dyadic Green's function $\overline{\boldsymbol{G}}^e_{pe}$ for the electric field produced by a unit electric current in the analysis region, we derive integral equations for the null condition of electric field on the post surface $S_{pi}(i = 1 - I_p)$

$$\int_{S_{pj}} ds_s \, \overline{\boldsymbol{G}}^e_{pe} \cdot \boldsymbol{J}_{pj} = \boldsymbol{0}. \tag{1}$$

In (1), $\overline{\boldsymbol{G}}^e_{pe}$ can be expanded in terms of $\pm x$-directed TE-to-z modes with the following wavenumber k_{zn} along the z direction according to Floquet's theorem:

$$k_{zn} = k_{zd} + 2n\pi/s \tag{2}$$

where n takes an integer number. Adopting Galerkin's method of moments in (1) yields a nonlinear equation for k_{zd} to obtain a nontrivial solution of $\boldsymbol{J}_{pj}$ in (1)

$$\det[Z_{ij}] = 0. \tag{3}$$

In (3), the components of the matrix are given as follows:

$$Z_{ij} = \int_{S_{pi}} ds_o \, \boldsymbol{J}_{pi} \cdot \int_{S_{pj}} ds_s \, \overline{\boldsymbol{G}}^e_{pe} \cdot \boldsymbol{J}_{pj}. \tag{4}$$

By solving (3) numerically, the complex numbers $k_{zd}(= k_{zdr} - jk_{zdi})$ are obtained. The real part k_{zdr} corresponds to the wavelength λ_f in the post-wall waveguide while the imaginary part k_{zdi} is associated with the leakage of the field toward the $\pm x$ directions.

Fig. 5 shows the width a_f as a function of the post spacing s to get the equal real part $k_{zdr}(= 1.206k_0)$ of the PEC wall waveguide for $a_e = 4.43$ mm. The other parameters are listed in Table I. When s increases, a_f decreases monotonously. This means that the inner field in the post-wall waveguide leaks intensively through the wider windows so that the equivalent PEC walls should be shifted outside. In Fig. 5, we also present the attenuation coefficient of the field. The attenuation is very

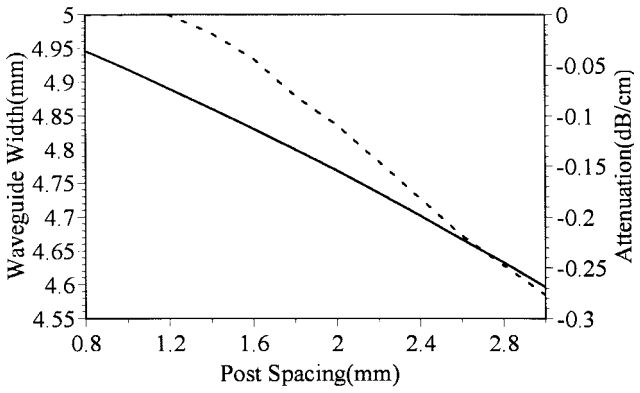

Fig. 5. Equivalent waveguide width and attenuation coefficient. —— equivalent waveguide width; ··· attenuation coefficient.

TABLE I
PARAMETERS OF THE FEED WAVEGUIDE

Equivalent Width of a Feed Waveguide	a_e	4.43mm
Spacing of Periodic Boundary Walls	a_r	6.30mm
Height of Parallel Plate Waveguide	b	1.52mm
Dielectric Constant	ε_r	2.17
Post Diameter	d	0.60mm
Distance of Additional Windows	h	1.70mm
Distance of a Short Circuit	e	2.50mm
Number of Pins per Post	I	12
Number of Basis Functions for Magnetic Current in Apertures		5
Frequency	f	40.0GHz

small for the post spacing up to 1.2 mm, i.e., twice the post diameter.

IV. ANALYSIS OF A PERIODIC WALL π JUNCTION

Let us consider the periodic wall π junction shown in Fig. 6 for incidence of the TE_{10} mode from Port 1. When the structure is 2-D and uniform to the y direction, the field in the junction can be expanded in terms of TE_{n0} modes. The analysis model is divided into three regions by placing PEC walls together with equivalent magnetic currents M_1, M_2 on the two apertures of the coupling windows according to the field equivalence theorem. The three regions are the feed waveguide (Region I), the wall-thickness (Region II), and the periodic wall waveguide (Region III). Several uniform electric currents are assumed on the surfaces of the reflection-canceling post ($\boldsymbol{J}_{rj}: j = 1 - I_r$), the waveguide post ($\boldsymbol{J}_{tj}: j = 1 - I_t$), and the window post ($\boldsymbol{J}_{wj}: j = 1 - I_w$), respectively [15], [16]. Next, applying the continuous conditions of the magnetic field on the window apertures (S_1 and S_2) and the null conditions of electric field on the PEC post surfaces (S_{ri}, S_{ti} and S_{wi}), we derive the coupled integral equations for electric and magnetic currents.

On S_{ri}

$$\boldsymbol{E}_{in} + \sum_{j=1}^{I_r} \int_{S_{rj}} ds_s \, \overline{\boldsymbol{G}}^e_{\mathrm{Ie}} \cdot \boldsymbol{J}_{rj} + \int_{S_1} ds_s \, \overline{\boldsymbol{G}}^e_{\mathrm{Im}} \cdot \boldsymbol{M}_1 = \boldsymbol{0}. \quad (5)$$

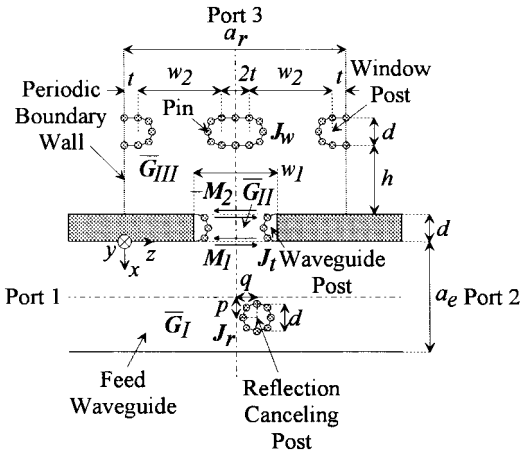

Fig. 6. Analysis model of a periodic wall π junction.

On S_1

$$\begin{aligned} \boldsymbol{H}_{in} + \sum_{j=1}^{I_r} \int_{S_{rj}} ds_s \, \overline{\boldsymbol{G}}^m_{\mathrm{Ie}} \cdot \boldsymbol{J}_{rj} + \int_{S_1} ds_s \, \overline{\boldsymbol{G}}^m_{\mathrm{Im}} \cdot \boldsymbol{M}_1 \\ = \int_{S_1} ds_s \, \overline{\boldsymbol{G}}^m_{\mathrm{IIm}} \cdot (-\boldsymbol{M}_1) + \sum_{j=1}^{I_t} \int_{S_{tj}} ds_s \, \overline{\boldsymbol{G}}^m_{\mathrm{IIe}} \cdot \boldsymbol{J}_{tj} \\ + \int_{S_2} ds_s \, \overline{\boldsymbol{G}}^m_{\mathrm{IIm}} \cdot \boldsymbol{M}_2. \end{aligned} \quad (6)$$

On S_{ti}

$$\begin{aligned} \int_{S_1} ds_s \, \overline{\boldsymbol{G}}^e_{\mathrm{IIm}} \cdot (-\boldsymbol{M}_1) + \sum_{j=1}^{I_t} \int_{S_{tj}} ds_s \, \overline{\boldsymbol{G}}^e_{\mathrm{IIe}} \cdot \boldsymbol{J}_{tj} \\ + \int_{S_2} ds_s \, \overline{\boldsymbol{G}}^e_{\mathrm{IIm}} \cdot \boldsymbol{M}_2 = \boldsymbol{0}. \end{aligned} \quad (7)$$

On S_2

$$\begin{aligned} \int_{S_1} ds_s \, \overline{\boldsymbol{G}}^m_{\mathrm{IIm}} \cdot (-\boldsymbol{M}_1) + \sum_{j=1}^{I_t} \int_{S_{tj}} ds_s \, \overline{\boldsymbol{G}}^m_{\mathrm{IIe}} \cdot \boldsymbol{J}_{tj} \\ + \int_{S_2} ds_s \, \overline{\boldsymbol{G}}^m_{\mathrm{IIm}} \cdot \boldsymbol{M}_2 \\ = \int_{S_2} ds_s \, \overline{\boldsymbol{G}}^m_{\mathrm{IIIm}} \cdot (-\boldsymbol{M}_2) + \sum_{j=1}^{I_w} \int_{S_{wj}} ds_s \, \overline{\boldsymbol{G}}^m_{\mathrm{IIIe}} \cdot \boldsymbol{J}_{wj}. \end{aligned} \quad (8)$$

On S_{wi}

$$\begin{aligned} \int_{S_2} ds_s \, \overline{\boldsymbol{G}}^e_{\mathrm{IIIm}} \cdot (-\boldsymbol{M}_2) \\ + \sum_{j=1}^{I_w} \int_{s_{wj}} ds_s \, \overline{\boldsymbol{G}}^e_{\mathrm{IIIe}} \cdot \boldsymbol{J}_{wj} = \boldsymbol{0}. \end{aligned} \quad (9)$$

In (5)–(9), $\boldsymbol{E}_{in}$ and $\boldsymbol{H}_{in}$ are the electric and magnetic field of the incident wave, while the dyadic Green's functions $\overline{\boldsymbol{G}}$'s are referred to as the following:

$\overline{\boldsymbol{G}}^e_{ke}$ for electric field produced by a unit electric current in Region k(k =I, II, and III);

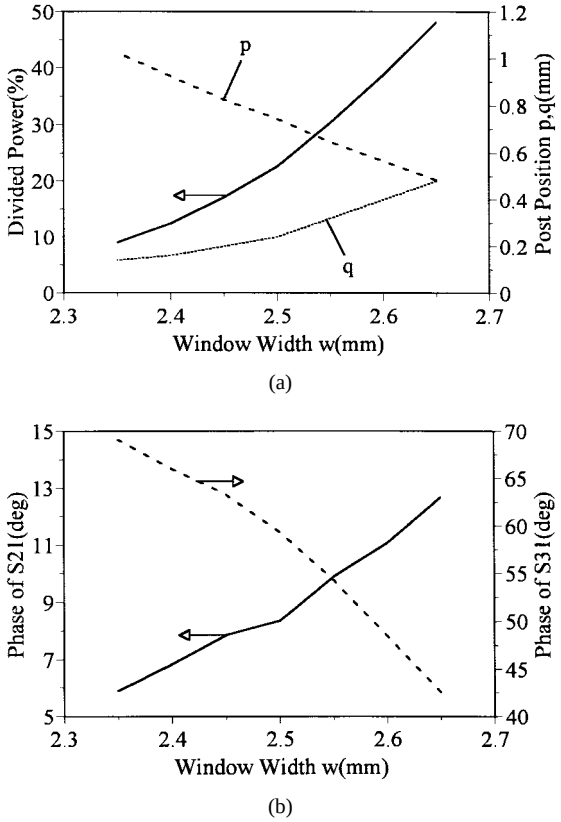

Fig. 7. Characteristics as functions of window width w_1. (a) Divided power (%) and post position (p, q). (b) Phase of S_{21} and S_{31} (deg).

$\overline{G}^m_{ke}$ for magnetic field produced by a unit electric current in Region $k(k$ = I, II, and III);

$\overline{G}^e_{km}$ for electric field produced by a unit magnetic current in Region $k(k$ =I, II, and III);

$\overline{G}^m_{km}$ for magnetic field produced by a unit magnetic current in Region $k(k$ =I, II, and III).

In the dyadic Green's functions of the periodic wall waveguide (Region III), the x dependence of the modes is expressed in terms of Fourier series with a period of a_r [14]. Galerkin's method of moments has then been applied to solve (5)–(9), where $\boldsymbol{M}_1$ and $\boldsymbol{M}_2$ have been expanded in terms of z-directed sinusoidal entire-domain basis functions [12]. Once $\boldsymbol{J}_{rj}$, $\boldsymbol{J}_{tj}$, $\boldsymbol{J}_{wj}$, $\boldsymbol{M}_1$, and $\boldsymbol{M}_2$ are obtained, the scattering matrix of the junction can be calculated.

V. Characteristics of Periodic Wall π Junctions

In order to design the feed waveguide, we have to investigate the dividing characteristics of the periodic wall π junction. Analyzing the dividing characteristics when the widths of both coupling and additional windows change, we have found that in-phase division with a desired power ratio can be obtained by controlling only the width w_1 of the coupling window and keeping the width w_2 of the additional one constant as shown in the next section. Therefore, w_2 is set to be a half of a_r so that the cross section of the window post is circular ($2t = 0$ in Figs. 3 and 5).

Fig. 7 shows characteristics of the junction as functions of the window width w_1. The other parameters are listed in Table I. The post position (p, q) is determined to suppress the reflection, below -40 dB for each w_1. In Fig. 7(a), the divided power becomes larger when the coupling window w_1 widens. The post should be placed close to the center $(p = 0)$ of the feed waveguide, where the electric field is strong for larger w_1 in order to cancel strong coupling of the window. It is shown in Fig. 7(b) that $\angle S_{21}$ has a small positive value since the effect of a series inductance of the coupling window on the TE_{10} mode transmission line is almost canceled by that of a parallel inductance of the reflection-canceling post [12].

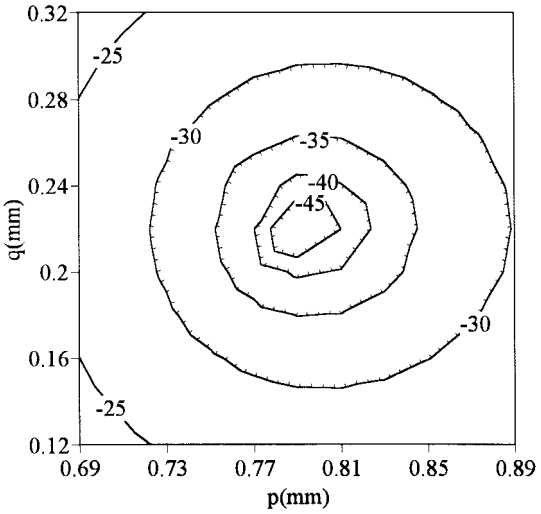

Fig. 8. Reflection (in decibels) as a function of post position ($w_1 = 2.45$ mm).

Fig. 8 depicts the contour map of the reflection as a function of the post position (p, q). About 20% of the divided power $|S_{31}|^2$ is obtained for $w_1 = 2.45$ mm. The reflection is minimized for $p = 0.79$ mm and $q = 0.22$ mm. This figure reveals the requirement on the accuracy of the post position to suppress the reflection. An $\pm$70-mm error is allowed in order to get reflection less than -30 dB.

VI. Design

At first, we briefly present a design of the feed waveguide allowing us to divide uniformly in both amplitude and phase into all the radiating waveguides. The followings are some guidelines to set the geometry of the feed waveguide properly.

1) The distance h of the additional windows from the coupling ones is set to be about 0.3–0.4 λ_r, where λ_r is the wavelength in the parallel plates.
2) The spacing a_r of the periodic boundary walls is set to be about 1.2–1.4 λ_r.
3) The equivalent width a_e of the feed waveguide is determined so that the guide wavelength λ_f of the feed waveguide is a bit shorter than a_r in order to compensate a 5–6° progression of the transmission phase $\angle S_{21}$ of the junction, as shown in Fig. 7(b).

The window width and the post position of each junction can be defined by the following procedures. N junctions are cascaded as shown in Fig. 9 and they are numbered from the termination to the input port. The desired divided power

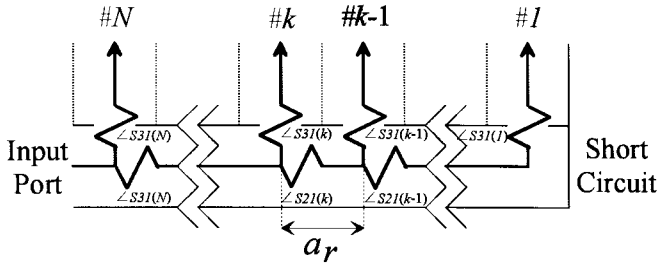

Fig. 9. Cascade of junctions.

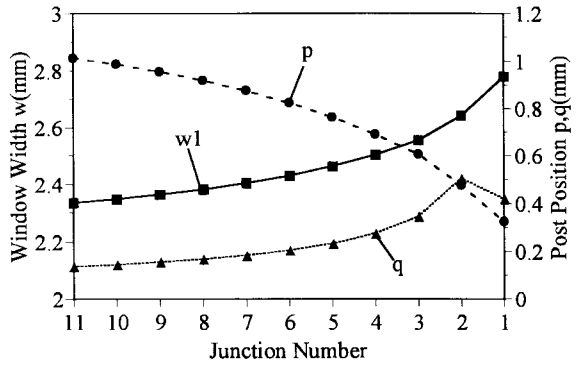

Fig. 10. Parameters of the feed waveguide.

$|S_{31}|^2$ of the junction $\#k(k = 1 - N)$ is $1/k$. The recursive equation for matching the phase $\angle S_{31}$ (deg) of the divided wave between the junctions $\#k - 1$ and $\#k$ is derived

$$\angle S_{31}(k) - 360 = \angle S_{21}(k) - a_r/\lambda_f \times 360 + \angle S_{31}(k-1). \quad (10)$$

According to the guideline 3) and (10), the phase difference of the divided wave between two adjacent junctions equals a few degrees and it is not necessary to control the phase $\angle S_{31}$ of the divided wave among the junctions in a wide range. $\angle S_{31}(k)$ of all the junctions can be evaluated by using (10) according to the design procedure described in [12], once $\angle S_{31}(1)$ of the junction #1 (matching junction) is given. Then all the parameters of the junction #k are obtained for $|S_{31}|^2(k)$ and $\angle S_{31}(k)$. A matching junction is designed for terminating the feed waveguide. Two posts are placed in the feed waveguide acting as an equivalent shorted circuit. The leakage from the two posts, i.e., the transmission S_{21}, is confirmed to be less than -30 dB. The coupling width $w_1(k)$ of each junction is determined from $|S_{31}|^2(k)$, $\angle S_{31}(k)$, and $\angle S_{21}(k)$ (shown in Fig. 7). Then post position $p(k)$ and $q(k)$ are obtained by using Fig. 7(a).

We design a cascade of eleven periodic wall π junctions. In this design, a_r/λ_f is fixed as 364.93°. Fig. 10 shows the parameters of the junctions. When the junction gets closer to the termination side, the width w_1 of the coupling window increases and the transverse position p of the reflection-canceling post shifts the center of the feed waveguide so that the divided power $|S_{31}|^2$ becomes larger. The matching junction #1 needs to compensate for 20° difference of the divided phase of the adjacent junction #2 by changing $w_1(1)$.

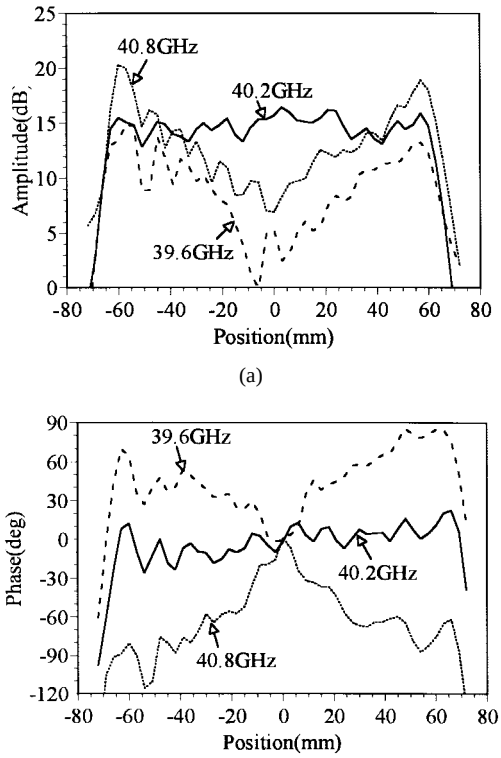

Fig. 11. Near-field distribution along the feed waveguide. (a) Amplitude. (b) Phase.

VII. Experimental Results

We have designed and fabricated a 40-GHz band model antenna using the feed waveguide. Fig. 11 shows the near-field distributions along the feed waveguide, which reflect on the dividing characteristics of the feed waveguide. The distribution is almost uniform in amplitude and phase at 40.2 GHz. The phase is tapered at the lower and higher frequencies due to the change in the wavelength in the feed waveguide. The amplitude was expected to be strong near the feed point (center) at the higher frequency, but it is actually strong near the edges of the feed waveguide. This may occur because of wave propagation along the array of the waveguide posts in front of the coupling windows.

The frequency bandwidth of the feed waveguide has been evaluated experimentally since we were not able to analyze the whole region. Fig. 12 demonstrates the frequency characteristic of a gain calculated by using the measured one-dimensional near-field distributions in Fig. 11. The 1-dB down bandwidth is about 3% (from 39.6 to 40.8 GHz).

VIII. Future Study

Practical realization of the desired performances of this feed waveguide depends on the accuracy of the post position. A numerical control machine to make via holes has typically ± 50-μm error in terms of the whole position. This position error of the posts composing the post-wall waveguide modifies the wavelength. The position error of the reflection-canceling post produces small reflection from each junction. As for a reflection-canceling post, an allowable error to suppress the reflection of a junction below -30 dB is estimated to be about

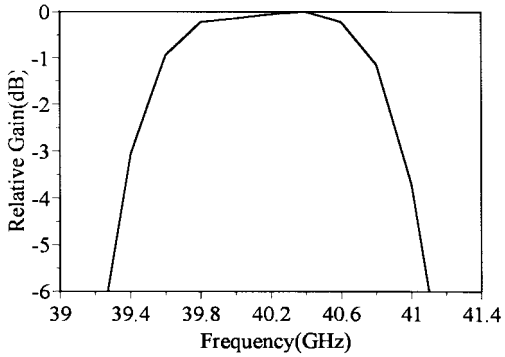

Fig. 12. Gain of near-field distribution.

± 15 μm in a 77-GHz band model for a car collision avoidance radar. Special fabrication techniques to reduce the position error will be required. We will investigate in detail the effects of this position error on the dividing characteristics, the bandwidth and the center frequency of the feed waveguide by analyzing the whole region. We will also evaluate conductor losses due to roughness of the surfaces of the metalized via holes.

After overcoming many problems still to be solved and realizing the desired performance of the feed waveguide, we will have to compare a planar antenna using this feed structure with a conventional antenna described in [10].

IX. Conclusion

The authors have proposed a single-layer feed waveguide to excite a plane TEM wave for parallel-plate slot arrays. The propagation constant of the post-wall waveguide has been calculated as a function of the spacing and the diameter of the posts. The inner field in the post-wall waveguide leaks intensively through the wider windows so that the equivalent PEC walls should be shifted outside. The attenuation is very small for the post spacing up to twice as long as the post diameter. The unit component named a periodic wall π junction has been analyzed by Galerkin's method of moments. The amplitude and the phase of the divided wave can be controlled by the width of the coupling window. A cascade of junctions has been designed to obtain an uniform division, which is confirmed by measurements on a 40-GHz band model. The 1-dB down bandwidth is about 3% in terms of the gain of the feed waveguide.

Acknowledgment

The authors would like to thank Prof. N. Goto of Takushoku University, Hachioji-shi, Japan, for his continuous fruitful suggestions.

References

[1] M. I. Skolnik, Ed., *Radar Handbook*. New York: McGraw-Hill, 1970, ch. 13.
[2] R. C. Johnson, Ed., *Antenna Engineering Handbook*, 3rd ed.. New York: McGraw-Hill, 1993, ch. 32.
[3] J. P. Quintez and D. G. Dudley, "Slots in a parallel plate waveguide," *Radio Sci.*, vol. 11, no. 8/9, pp. 713–724, Aug./Sept. 1976.
[4] T. L. Keshavamurthy and C. M. Butler, "Characteristics of a slotted parallel-plate waveguide filled with a truncated dielectric," *IEEE Trans. Antennas Propagat.*, vol. AP-29, pp. 112–117, Jan. 1981.
[5] H. A. Auda, "Quasistatic characteristics of slotted parallel-plate waveguide," *Proc. Inst. Elect. Eng.*, vol. 135, pt. H, no. 4, pp. 256–262, Aug. 1988.
[6] Y. K. Cho, "On the equivalent circuit representation of the slotted parallel-plate waveguide filled with a dielectric," *IEEE Trans. Antennas Propagat.*, vol. 37, pp. 1193–1200, Sept. 1988.
[7] Y. Wagatsuma and T. Yoneyama, "Multiply folded sectoral horn fed planar antenna," in *Proc. Communicat. Conf. Inst. Electron. Inform. Commun. Eng.*, Tokyo, Japan, B-1-53, Sept. 1996.
[8] M. Sato, Y. Konishi, and S. Urasaki, "A traveling-wave fed slot array antenna with inclined linear polarization at 60-GHz band," in *Proc. Communicat. Conf. Inst. Electron. Inform. Commun. Eng.*, Tokyo, Japan, B-1-68, Sept. 1996.
[9] Y. Wagatsuma, Y. Daicho, and T. Yoneyama, "Leaky NRD-guide fed folded planar antenna," in *Proc. Gen. Conf. Inst. Electron. Inform. Commun. Eng.*, Tokyo, Japan, B-1-177, Mar. 1997.
[10] J. Hirokawa, M. Ando, and N. Goto, "Waveguide-fed parallel plate slot array antenna," *IEEE Trans. Antennas Propagat.*, vol. 40, pp. 218–223, Feb. 1992.
[11] N. Goto, "A planar waveguide slot antenna of single layer structure," Inst. Electron. Inform. Commun. Eng., Tokyo, Japan, Tech. Rep. AP88-39, July 1988.
[12] J. Hirokawa, M. Ando, and N. Goto, "A single-layer multiple-way power-divider for a planar slotted waveguide array," *IEICE Trans. Commun.*, vol. 75, no. 8, pp. 781–787, Aug. 1992.
[13] N. Goto, "A technique of grating lobe suppression and an application to planar waveguide slot arrays for dual frequency use," Inst. Electron. Inform. Commun. Eng., Tokyo, Japan, Tech. Rep. AP87-10, May 1987.
[14] J. Hirokawa, M. Ando, and N. Goto, "Analysis of slot coupling in a radial line slot antenna," *Proc. Inst. Elect. Eng.*, vol. 137, pt. H, no. 5, pp. 249–254, Oct. 1990.
[15] Y. Leviatan, P. G. Li, A. T. Adams, and J. Perini, "Single-post inductive obstacle in rectangular waveguide," *IEEE Trans. Microwave Theory Tech.*, vol. MTT-31, pp. 806–812, Oct. 1983.
[16] H. Auda and R. F. Harrington, "Inductive posts and diaphragms of arbitrary shape and number in a rectangular waveguide," *IEEE Trans. Microwave Theory Tech.*, vol. MTT-32, pp. 606–613, June 1984.

Jiro Hirokawa (S'89–M'90) was born in Tokyo, Japan, on May 8, 1965. He received the B.S., M.S., and D.E. degrees in electrical and electronic engineering from Tokyo Institute of Technology, Tokyo, Japan, in 1988, 1990, and 1994, respectively.

From 1990 to 1996, he was a Research Associate and is currently an Associate Professor at Tokyo Institute of Technology. From 1994 to 1995, he was with the antenna group of Chalmers University of Technology, Gothenburg, Sweden, as a Postdoctoral Researcher on leave from the Tokyo Institute of Technology. His research interest has been in the analysis of slotted waveguide array antennas.

Dr. Hirokawa received the Young Engineer Award from IEICE Japan in 1996.

Makoto Ando (M'83) was born in Hokkaido, Japan, on February 16, 1952. He received the B.S., M.S., and D.E. degrees in electrical engineering from Tokyo Institute of Technology, Tokyo, Japan in 1974, 1976, and 1979, respectively.

From 1979 to 1983, he worked at Yokosuka Electrical Communication Laboratory, NTT, Yokosuka-shi, Japan, and was engaged in the development of antennas for satellite communication. He was a Research Associate at Tokyo Institute of Technology from 1983 to 1985 and is currently a Professor there. His main interests have included high-frequency diffraction theory such as physical optics and geometrical theory of diffraction, the design of reflector antennas and waveguide planar arrays for direct broadcast from satelite (DBS) and very small aperture terminal (VSAT), and the design of high-gain millimeter-wave antennas.

Dr. Ando received the Young Engineers Award of IECE Japan in 1981 and the Achievement Award and the Paper Award from IEICE Japan in 1993. He also received the fifth Telecom Systems Award in 1990 and the eighth Inoue Prize for Science in 1992.